doi:10.1088/1742-6596/59/1/057 Eighth International Conference on Laser Ablation

# Concentrating light into nanometer domain using nanoscale ridge apertures and its application in laser-based nanomanufacturing

**X Xu, E X Jin, S M Uppuluri and L Wang**

School of Mechanical Engineering
Purdue University
West Lafayette, IN 47907
USA

E-mail: xxu@ecn.purdue.edu

**Abstract**. In this work, we investigate light concentration in nanoscale ridge apertures and its applications in nanomanufacturing. Optical transmission of ridge apertures in a metal film is optimized by numerical design using the finite-difference time-domain (FDTD) method. We show that ridge apertures provide an optical transmission enhancement of several orders of magnitude higher than regularly shaped nanoscale apertures, and also confine the transmitted light to nanoscale dimensions. We fabricated these ridge apertures in metal film coated on quartz substrates by focused ion beam (FIB) milling. These apertures are characterized by near-field scanning optical microscopy (NSOM). The ridge apertures are also used as a nanoscale light source for nanolithography. Holes with sub-100 nm dimensions are produced in the photoresist with visible and UV laser illuminations. The performance of the ridge apertures is compared with that of regular nanoscale apertures to demonstrate their advantages and promising potentials for many near-field optical applications.

## 1. Introduction

The ability of manipulating light at an extremely small spatial scale is of great importance to the continuous miniaturization of electronic, optical and optoelectronic devices. A subwavelength hole in an opaque screen can be used to provide a small light source with the optical resolution beyond the diffraction limit in the near field [1]. However, a nanometer-sized hole in circular or square shapes suffers low light transmission [2-3] at visible wavelengths due to the cutoff effect [4]. For a subwavelength circular hole in a thin and perfect conductor screen, the light transmission coefficient is proportional to the fourth power of the ratio of the diameter of the hole to the light wavelength [2]. This low transmission limits the nanoscale apertures from being employed in many practical applications.

The utilization of an array of holes [5] or a single hole surrounded by periodic structures [6] in noble metals shows transmission enhancement with the aid of the resonant excitation of surface plasmon (or surface modes), while the spatial resolution is somehow sacrificed by the period of the hole array. Ridge apertures in C, H and Bowtie shapes [7-11], on the other hand, have been numerically demonstrated to show the ability of achieving both enhanced light transmission and subwavelength optical resolution based on the finite-difference time-domain (FDTD) computations. In

© 2007 IOP Publishing Ltd

addition, both light concentration [12] and transmission enhancement [13] through C-shaped ridge apertures have been reported experimentally and shown to be consistent with the numerical predications.

One of the important nanotechnologies is the nanomanufacturing or nanolithography. Nanolithography techniques such as scanning probe lithography [14] and nanoimprint lithography [15] have been proposed as alternatives for high cost nanopatterning methods such as e-beam or X-ray lithography. It has also been demonstrated that light enhancement in the near field of various structures can be used for nanolithography applications. For examples, evanescent near-field optical lithography shows the capability of making sub-100 nm gratings on photoresist [16]. The excitation of surface plasmon through the periodic hole arrays also has been utilized for nanoscale contact lithography [17, 18]. In this paper, we will show that the ridge nano-aperture is promising for low cost and high efficiency nanolithography and nanomanufacturing due to its intrinsic advantages of achieving enhanced optical transmission through a single aperture and concentrating light far beyond the diffraction limit without resorting to the expensive deep or extreme ultraviolet sources of shorter wavelengths. The optimal design of a ridge nanoaperture for nanolithography application will be discussed, followed by fabrication of the nanoapertures using focused ion beam (FIB) milling. The optical near-field properties of fabricated nanoapertures are characterized by near-field scanning optical microscopy (NSOM). Finally, the ridge nanoapertures are applied for near-field nanolithography to demonstrate their superior capabilities in terms of enhanced light transmission and light concentration compared to conventional apertures.

## 2. Optimal Design of Ridge Nanoapertures

The ridge aperture adopts the concept of ridge waveguide in microwave engineering [19] while having nanoscale dimensions and operating in the optical regime. As shown in Figure 1, ridge apertures have two common features: (1) two open arms and (2) a narrow gap. The nanometer-sized gap concentrates the light through ridge aperture to a nanoscale light spot in the near field, and the open arms endow the ridge aperture with long cutoff property which enables the propagation waveguide mode in the aperture, even for visible wavelengths, therefore boosting the transmitted light [9]. In order to reach the best performance for a ridge nanoaperture in the application of nanolithography, it is important to optimize nanoaperture designs to achieve maximum power throughput and obtain the desired nanoscale features.

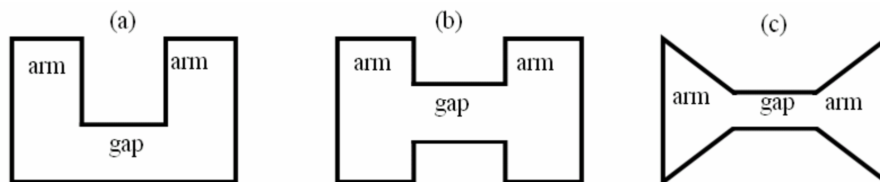


**Figure 1.** Schematic view of ridge apertures in (a) C, (b) H and (c) bowtie shapes.

The gap size of the ridge aperture to be designed is determined by the desired optical resolution. For example, a C aperture with a gap of 60 nm × 60 nm could provide a light spot as small as 80 nm × 80 nm at 25 nm below the aperture to the first order approximation. The optimal geometry of a ridge aperture is obtained by computing and analyzing the spectrum response of the designed aperture [20] and tuning the geometric size of the aperture so that the intrinsic resonant wavelength matches to the laser wavelength. It is also important to choose the right metal as the material of the opaque film, as it should have high reflection (to suppress the background light transmission through the metal film) and small skin depth (less loss for the light propagating through the aperture) [11]. For example, at an argon-ion laser wavelength of 458 nm, it turns out that aluminum could be suitable (refractive index $n = 0.65 + 5.6j$, dielectric constant $\varepsilon = -30 + 7.3j$, reflectivity $R = 0.92$, skin depth $\delta = 6.5$ nm) for the film material. The aluminum film should be thick enough to completely block the background light in

order to have a good contrast between the transmitted light propagated through the aperture and that penetrated through the film. In addition, the film thickness can be optimized to satisfy the Fabry-Pérot-like resonance condition to boost the transmission further [9].

Implementing these strategies, we have designed C aperture with dimensions $a$ = 160 nm, $b$ = 110 nm, $s$ = 60 nm, and $d$ = 60 nm, in a $t$ = 150 nm thick aluminum film using FDTD simulations, which shows a resonance wavelength at 465 nm, close to the design wavelength $\lambda$ = 458 nm. Resonant H aperture with similar dimensions has also been designed. Figure 2(a) shows the light propagation through the designed C aperture in the cross section along the dash line shown in Figure 2(b). An 82 nm × 76 nm near-field spot (calculated) is obtained at 25 nm below the aperture as shown in Figure 2(b). The transmission efficiency for the designed C aperture, normalized to the aperture area, is calculated to be 0.88. A small square aperture (60 nm by 60 nm), which can provide the near-field spot of the same size as that obtained from the C aperture, only has a transmission efficiency of $1.8 \times 10^{-5}$. Therefore, the C aperture has the enhanced transmission four orders of magnitude higher than the comparable regular aperture. For the large square aperture (120 nm by 120 nm) of the same opening area, although its transmission efficiency is 0.023, it is not able to provide a sub-100 nm near-field spot. Compared to regular apertures of common shapes, a resonant ridge aperture can efficiently collect photons from an area outside the aperture, concentrate the collected photons into the gap region and deliver them to the exit side of the aperture through the propagation waveguide mode.

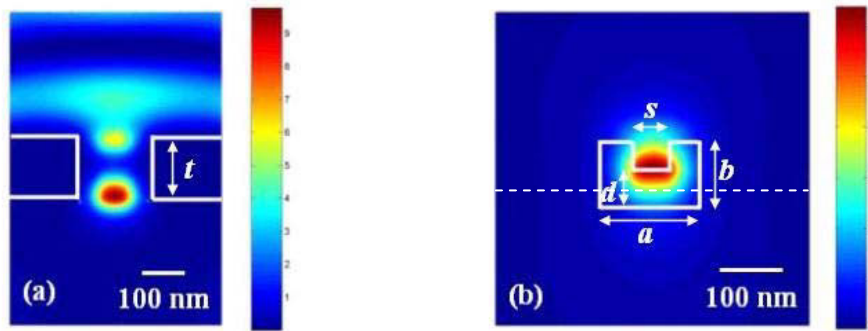


**Figure 2.** FDTD computation shows (a) the 458 nm light propagation through a designed C aperture in the cross section along the dash line in (b) the transmitted light at 25 nm below the C aperture in a 150 nm thick aluminum film.

### 3. Optical Characterization of Nanoapertures by Near-field Optical Scanning Microscopy

To prepare the aperture sample for the optical characterization, optically flat quartz substrates are first deposited with 150 nm aluminum film. Ridge nanoapertures in C and H shapes with the designed dimensions are subsequently fabricated on the aluminum film by exposing with Ga+ ions from a dual beam FIB machine. Square-shaped regular apertures with the similar overall opening areas or having the same size of the gap area as those of ridge apertures are also fabricated on the same sample for comparison. Figure 3 shows the SEM images of the fabricated nanoapertures.

The optical transmission of the fabricated nanoapertures is investigated using a home-built near-field scanning optical microscope. The ridge aperture is illuminated by an argon-ion laser ($\lambda$ = 458 nm) from the substrate side. The incident laser beam is focused on the metal film and the light needs to be polarized in the direction across to the ridges [9]. A cantilever-typed NSOM probe with sub-100 nm aperture at the apex (not shown here), which gives the spatial resolution of about 60 nm, is brought to the close proximity of the surface, and then in soft contact with the surface to collect the transmitted light through the nanoapertures. The soft contact between the probe and sample surface is controlled by a commercial AFM module based on the cantilever beam deflection technique.

The NSOM images shown in Figure 4 are obtained after raster-scanning the probe over each aperture and collecting the transmitted light signal through the aperture probe in the far field with a photomultiplier tube (PMT). As shown in the figure, the full-width half-magnitude (FWHM) of the near-field light spots scanned over C, H and large square apertures are found to be 86 nm × 90 nm, 72

nm × 103 nm, and 124 nm × 128 nm respectively. The NSOM measurement of the smaller square aperture of the size of 60 nm × 60 nm is also attempted but failed to have enough light signal that can be detected. Due to the resolution limitation of the aperture probe that is used for the measurements, the actual spot size from the C and H apertures could be smaller.

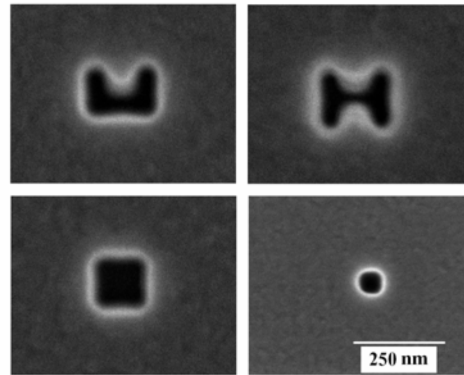


**Figure 3.** SEM images of ridge apertures and regular apertures fabricated in aluminum film for the optical characterization.

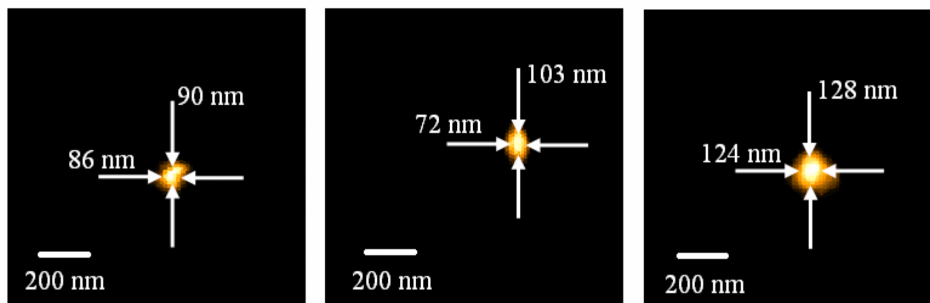


**Figure 4.** Near-field scanning optical microscopy images obtained by C (a), H (b) and large square (c) apertures shown in figure 3.

Figure 4 demonstrates that both C and H apertures are able to concentrate light to a sub-100 nm scale optical spot with enhanced transmission compared to the small square aperture, which has the same size as the gap of the C and H apertures. Although a quantitative transmission comparison between the ridge apertures and the large square aperture with a similar opening area is difficult to perform because of the finite aperture size of the scanning NSOM probe and its interaction with the transmitted light, the measured NSOM spot through the square aperture is larger than those of ridge apertures in both directions, which shows the advantage of using ridge apertures to concentrate light.

## 4. Nanolithography Using Ridge Apertures

C-shaped ridge apertures are tested for nanolithography applications. The design wavelengths are 355 nm and 458 nm. Square aperture (SA) and rectangular aperture (RA) with the same opening area as that of the C aperture, small square aperture (SG) of the same size as the gap and rectangular aperture (OU) with dimensions corresponding to the outer edge dimensions of the C aperture are made in an array pattern for convenient comparison. Figure 5 shows the SEM image of one aperture array.

Figure 6 shows the schematic diagram of the experimental lithography setup. The experimental setup is housed in a class-10 glove box and screened from white light in order to avoid contamination

and photoresist exposure. The aperture mask is held in contact with the positive photoresist (Shipley S1805) coated quartz sample during the lithography experiments. A diode pumped solid state (DPSS) laser at 355 nm wavelength and an argon-ion laser at 458 nm with linear polarization are used as the light sources for exposure. The laser polarization needs to be directed perpendicular to the ridge of the C aperture [9].

Lithography experiments were first performed by using the 458 nm argon-ion laser and it was found that sensitivity of the photoresist is not good enough to produce the expected results due to the fact that S1805 photoresist is not optimized for 458 nm. Extensive lithography experiments are therefore conducted using 355 nm DPSS laser exposure.

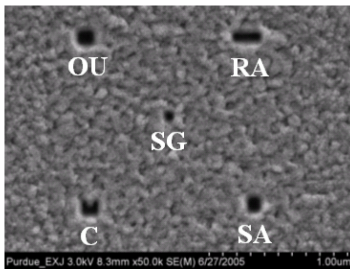


**Figure 5.** SEM picture of the lithography mask pattern: C aperture with 120 nm × 100 nm outline and 50 nm × 50 nm gap is fabricated on aluminum thin film. Comparable apertures are made on the array pattern based on the C aperture: 100 nm × 100 nm square aperture (SA) and 200 nm × 60 nm rectangular aperture (RA) of the same opening area, 120 nm × 100 nm aperture (OU) of the same outline, and 50 nm × 50 nm square aperture (SG) of the same gap size.

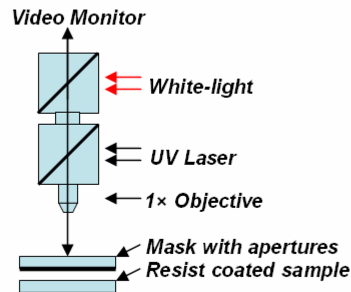


**Figure 6.** Schematic diagram of the experimental lithography setup.

Different exposure doses are employed by varying the exposure time while maintaining a fixed laser output power. By reducing the exposure time, it is found that SA aperture stops giving any results first, then OU aperture start to produce partially developed shallow hole as shown in the AFM image of the lithography results in Figure 7. SG aperture does not give any results at any tested exposure time and RA aperture always produces holes larger than 150 nm. Only C aperture produces the sub-100 nm hole (shown in figure 8).

The above lithography results demonstrate C aperture has better transmission than the SG, SA and OU apertures owing to the existence of the waveguide propagation mode in the C aperture. Since the cutoff wavelength of RA aperture is longer than 355 nm, the propagation mode is also excited in the RA aperture, therefore enabling higher power throughput than the other regular apertures. However, it is not able to produce sub-100 nm feature.

## 5. Conclusions

In conclusion, ridge nanoapertures have been designed using FDTD simulations and fabricated by the FIB nanopatterning technique. Near-field optical spots transmitted through ridge apertures and comparable regular apertures have been characterized by NSOM measurements to show the light concentration function of ridge apertures. Nanolithography experiments have been performed to demonstrate the advantages of ridge apertures over conventional apertures in both transmission enhancement and nanoscale light concentration. These ridge apertures should have potentials in other

near-field applications such as ultrahigh density optical or magnetic data storage and nanoscale imaging.

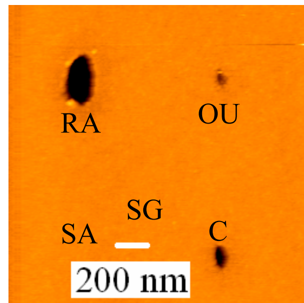


**Figure 7.** AFM topography of lithography results when OU aperture begins to be partially developed.

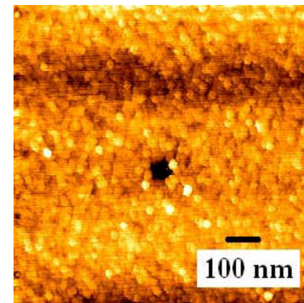


**Figure 8.** AFM image of 50 nm × 60 nm hole produced by C aperture.

**Acknowledgements**
Supports to this work by the Office of Naval Research and the National Science Foundation are acknowledged. Fabrications of aperture samples by FIB were carried out in the Center for Microanalysis of Materials, University of Illinois, which is partially supported by the U.S. Department of Energy under grant DEFG02-91-ER45439.

**References**

[1] Synge E H 1928 *Philos. Mag.* **6** 356.
[2] Bethe H A 1944 *Phys. Rev.* **66** 163.
[3] Leviatan Y 1986 *J. Appl. Phys.* **60** 1577.
[4] Rayleigh L 1897 *Philos. Mag.* **43** 125.
[5] Ebbesen T W, Lezec H J, Ghaemi H F, Thio T, and Wolff P A 1998 *Nature* **391** 667.
[6] Thio T, Pellerin K M, Linke R A, Lezec H J, and Ebbesen T W 2001 *Opt. Lett.* **26** 1972.
[7] Shi X and Hesselink L 2002 *Jpn. J. Appl. Phys.* **41** 1632.
[8] Sendur K and Challener W 2003 *J. of Microscopy* **210** 279.
[9] Jin E X, and Xu X 2004 *Jpn. J. Appl. Phys.* **43** 407.
[10] Jin E X, and Xu X 2004 2005 *J. of Quantitative Spectroscopy and Radiative Transfer* **93** 163.
[11] Jin E X, and Xu X 2004 2005 *Appl. Phys. Lett.* **86** 111106. Also appear in the March 21, 2005 issue of *Virtual Journal of Nanoscale Sci. & Tech.*
[12] Chen F, Itagi A, Bain J A, Stancil D D, Schlesinger T E, Stebounova L, Walker G C, and Akhremitchev B B 2003 *Appl. Phys. Lett.* **83** 3245.
[13] Matteo J A, Fromm D P, Yuen Y, Schuck P J, Moerner W E, and Hesselink L 2004 *Appl. Phys. Lett.* **85** 648.
[14] Marrian C R K and Colton R J 1990 *Appl. Phys. Lett.* **56** 755.
[15] Chou S Y, Krauss P R and Rentstrom P J 1995 *Appl. Phys. Lett.* **67** 3114.
[16] Alkaisi M M, Blaikie R J, McNab S J, Cheung R and Cumming D R S 1999 *Appl. Phys. Lett.* **75** 3560.
[17] Luo X and Ishihara T 2004 *Appl. Phys. Lett.* **84** 4780.
[18] Srituravanich W, Fang N, Sun C, Luo Q and Zhang X 2004 *Nano Lett.* **4** 1085.
[19] Helszajn J, 2000 Ridge waveguides and passive microwave components, IEE, London.
[20] Shi X and Hesselink L, 2004 *J. of the Opt. Soc. of Ame. B* **21** 1305.